Charging/Discharging of Thin PS/PMMA Films As Probed by Dynamic X-ray Photoelectron Spectroscopy

Hikmet Sezen,[†] Gulay Ertas,[†] Aykutlu Dâna,[‡] and Sefik Suzer*,[†]

Departments of Chemistry and Physics, Bilkent University, 06800 Ankara, Turkey

Introduction. Use of polymeric materials for coating applications is ever increasing due to ease of controlling their morphology, flexibility, friction and wetting, etc., properties, through surface engineering.[1−7] Functionality is usually improved by using more than one component through blending, and the resultant surface composition of a polymer blend is primarily controlled by the difference in surface free energy of each component, molecular weight, end groups, and architecture. When the films are cast form solution, the nature of the solvent is another important factor controlling the surface composition. For example, it was reported that the surface was enriched with PMMA if blends were cast from THF, while surface composition was equivalent to that of bulk if blends were cast from MEK for PVC/PMMA blends.[8] PS/PMMA is one of the extensively studied immiscible combination for which bulk and surface phase separation has been observed using a variety of conditions.[1,9−14] The nature of the substrate also affects the surface morphology. For thick films (25 μm), a PS-rich overlayer was formed, and the surface morphology was not influenced by the substrate characteristics.[1] In the case of ultrathin films (10 nm), neither dependence on substrate characteristics nor phase separation was detected. For films of 100 nm thicknesses, both phase-separated structures at the film surface and substrate dependence were observed. The PMMA domain size and shape were dependent on substrate, and an increase in substrate hydrophilicity decreased the PMMA concentration on the surface of the film. Similar results were obtained for PS/PMMA blends from solutions in THF.[12] The effect of chain ends is also important in surface morphology. If the surface free energy is lower for the end groups than for the main chain part, the end groups are preferentially located at the surface;[15,16] this explains a possible influence of the molecular mass. PMMA with a very low molecular mass compared to PS was preferentially segregated at the film surface, although it has a higher surface energy than PS.[17] In addition, surface fraction of the PMMA decreased with an increase of PMMA molecular mass. Lateral domains with a well-defined surface structure can be obtained by spin-coating a film of immiscible polymers from a common solvent. These structures were essentially determined by the different solubilities of the two polymers in their common solvents[18] and the varying substrate preferences of the two polymers.[1,12]

The surface compositions of blends have been extensively characterized using XPS, SIMS, FTIR, neutron reflectivity, and contact angle goniometry. AFM is commonly used for structural characterization in the nanometer scale,[15,19−22] Sum−difference frequency spectroscopy has also been applied for investigation of polymer surfaces and interfaces.[23,24]

XPS is an excellent technique for determining chemical composition of surface layers of 1−10 nm,[3,4,8−10,25] but one of the frequently encountered problems in XPS analysis of polymeric surfaces is differential charging, which is usually considered as a nuisance.[26] However, this has recently been utilized for detecting surface phase separation in the immiscible blends of poly(sebacic anhydride) and poly(DL-lactic acid).[3] Similarly, we have been utilizing this differential charging in analyses of various surface structures for characterizing phase separation and/or other properties of organic/inorganic systems.[27−29] We have also shown that electrical parameters like resistance and/or capacitance can also be extracted using dynamical XPS measurements.[28,30] In this study, we extend our technique to analysis of thin (10−50 nm) PS/PMMA films both for detecting phase separation as well as probing their electrical responses by XPS.

Experimental Section. A Kratos ES300 electron spectrometer with Mg Kα X-rays (nonmonochromatic) is used for XPS measurements, and a nearby filament provides low-energy electrons for charge neutralization. The polymers used in this work are PS and PMMA, purchased from Aldrich. Polymer solutions, prepared by dissolving in chlorobenzene, are used for making films by spin-casting onto Si(100) substrates. Chlorobenzene is chosen since it is known not to have a strong influence on the surface composition.[18] Average thicknesses of the films are measured using a stylus profilometer. For probing charging or electrical properties, the sample rod is subjected either to ±10 V dc stress or to square-wave pulses (SQW) of ±10 V amplitude with varying frequencies in the $10^{-3}-10^{3}$ Hz range, while recording XPS data. We have also developed a simple model, treating a homogeneous surface layer as consisting of a serious resistor (R) and a parallel capacitor (C), for calculating the dynamic behavior of surface structures.[30]

Results and Discussion. When the sample is subjected to external dc stress, the positions of the peaks shift to lower or higher binding energies, since their kinetic energies are increased ($-ve$ stress) or decreased ($+ve$ stress), respectively. Accordingly, for a conducting sample (i.e., graphite) the shifts are exactly +10 eV or −10 V due to the absence of charging. However, the shifts are smaller than 10 eV for a nonconducting sample because of the development of electrical potentials due to charging. Polarity of the voltage stress is another parameter affecting charging, since when a negative stress is applied to the sample, neutralizing low-energy electrons are repelled to result in development of a higher positive charge. Under a positive stress, low-energy electrons are attracted to the sample and yield less positive charge on the sample, due to partial neutralization. The extent of these shifts (differences from 10 eV) is also different for PS and PMMA of comparable thickness due to differences in charging properties of these polymer, as shown in Figure 1b,c. More interestingly, for the blend sample the peaks (both C 1s and O 1s) become broader, again due to different extent of charging of the separate phases of PS and PMMA domains, as displayed in the inset to Figure 1b for the C 1s region, where the peaks belonging to PMMA and to PS are separated from each other, especially under −10 V stress. We would like to emphasize that this is a very clear spectroscopic evidence of phase separation.[29]

* Corresponding author. E-mail: suzer@fen.bilkent.edu.tr.
† Department of Chemistry.
‡ Department of Physics.
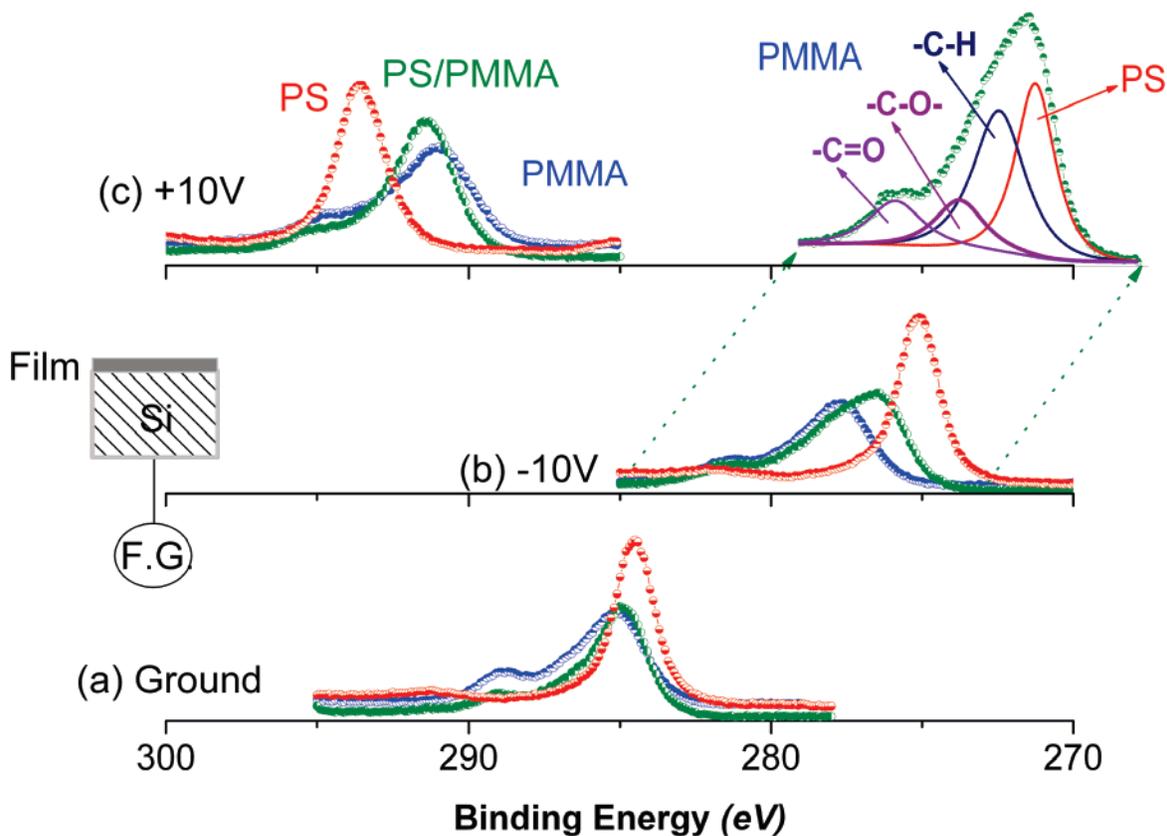
Figure 1. XPS spectra of the C 1s regions of films of PS (ca. 20 nm), PMMA (ca. 20 nm), and a 50% blend (ca. 15 nm), recorded when (a) grounded, (b) subjected to −10 V, and (c) to +10 V voltage stress. PS and PMMA films are shifted differently due to the extent of differential charging, and the shifts for the blend film are in between. Phase separation is clearly observable as shown in the inset. Peaks belonging to PMMA and to PS exhibit different charging behavior due to their different chemical and electrical properties. The inset schematically shows the connection of the function generator (F.G.) to the sample.

When the sample is subjected to SQW pulses with varying frequencies, more detailed information can be extracted. For example, when the XPS spectrum of a conducting sample of graphite is recorded, the peaks appear respectively at −10 and +10 eV binding energies (i.e., with exactly 20.0 eV difference between them) at all frequencies, since the sample spends 50% of its time at −10 and +10 V, respectively, as shown in Figure 2a. However, for the ca. 20 nm PS film, the corresponding peaks are separated by less than 20 eV due to differential charging of the polymeric coating. Moreover, the measured binding energy difference exhibits a strong frequency dependence, as shown in Figure 2b.

This charging behavior of thin polymeric films can experimentally be mimicked by connecting an external series resistor and a parallel capacitor (e.g., 8.2 Mohm + 1.0 μF) to the conducting graphite sample, as shown in Figure 3a. In the absence of the RC, the C 1s peaks of the graphite are separated by 20.0 eV at all frequencies. After connecting through the RC, and at low frequencies, separation between the peaks becomes smaller than 20.0 eV, since enough time is given to the system (RC) to charge and discharge, and introduces an additional potential due to the IR drop. At high frequencies the system recovers, and again 20.0 eV difference is measured. The similarity between graphite + RC and the ca. 20 nm PS film as far as their response to electrical stress with varying frequencies is concerned, is clearly depicted in Figure 3b. Accordingly, a 20 nm PS layer responds as if having ca. 9.5 Mohm resistance and 1.6 μF capacitance, which is also plotted as our calculated results.[30]

Under the same conditions, a thicker sample of ca. 55 nm PS reacts as if having a higher resistance (ca. 50 Mohm), but a
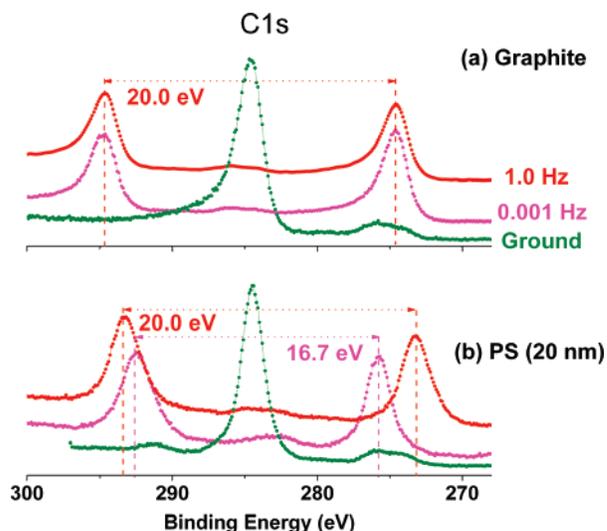

Figure 2. (a) C 1s spectrum of graphite recorded, when grounded (olive), and when subjected to ±10 V SQW pulses of 0.001 Hz (magneta) and 1.0 Hz (red). Because of the conducting nature of graphite, the peaks are separated by 20.0 eV at all frequencies. (b) Spectra recorded under SQW pulses of 0.001 Hz (magneta) and 1.0 Hz (red) of a ca. 20 nm PS film on a silicon wafer. Charging is evidenced due to smaller than 20.0 eV difference between the peaks at low frequencies.

proportionally smaller (ca. 0.34 μF) capacitance with almost the same RC time constant of 17 s, as shown in Figure 4a, again together with our calculated data. For a thin film of PMMA longer and a distinctly different time constant (200 s) is measured as shown in Figure 4b. Hence, dynamically measured
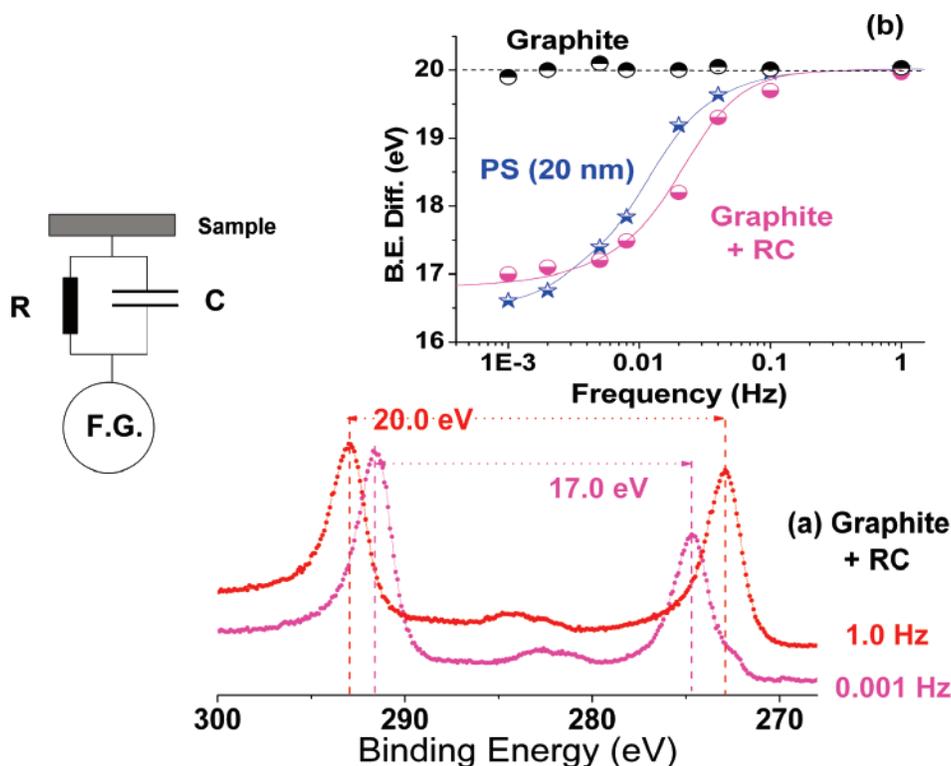
Figure 3. (a) Spectra recorded when the graphite sample is connected through an external RC circuit (8.2 Mohm, 1.0 μF), as schematically shown in the inset, to create a charging system artificially; under SQW pulses of 0.001 Hz (magneta) and 1.0 Hz (red). (b) Dependence of the measured B.E. difference on the frequency of the SQW stress for graphite only, graphite + RC, and ca. 20 nm PS only, together with our calculated data.
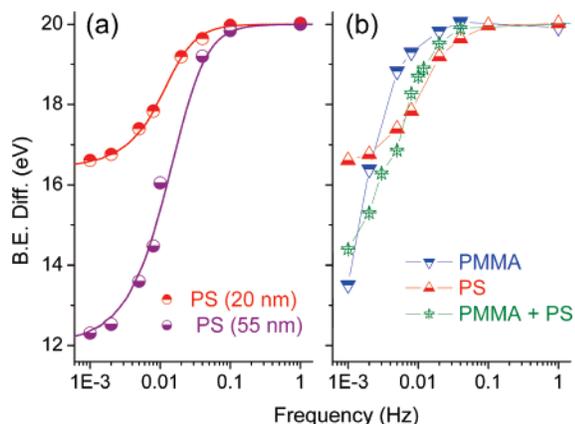
Figure 4. Frequency dependence of the measured difference between the peaks shown in Figure 2 for (a) two PS films of 20 and 55 nm thickness, (b) one PS (20 nm), one PMMA (20 nm) and one PS/PMMA blend (15 nm) film. Solid lines are our calculated data.

RC values seem to be very specific to the nature of the polymer. This also manifests itself in the blend film of 50% PS and 50% PMMA spin-cast from chlorobenzene solution, as depicted in Figure 4b, for three films (PS only, PMMA only, and PS + PMMA blend) of comparable thickness. The blend displays a frequency dependence which is almost a hybrid mixture of the two components.

To our knowledge, this is the first time such dynamical XPS measurements have been conducted for the purpose of extracting electrical parameters of thin polymeric materials. Considering the multitude of the parameters affecting the electrical properties of polymeric films (tacticity, packing, crystalinity, defect density, etc.), it is surprising that the response of these films to SQW stresses can be fitted by a simple single R and a single C value. Second, there are also many different forms of the electrical stress besides the simple SQW we have adopted in this study

for probing dynamical responses of polymeric films. Finally, whether or not the extracted R and C values using our method can be related to some intrinsic properties of these films are important questions yet to be answered, but definitely worth pursuing.

Conclusions. We demonstrate that, by subjecting the samples to external dc and/or ac pulses, while recording XPS data, it is possible to extract electrical parameters with chemical specificity of thin polymeric materials. Our technique is simple and versatile which turns the powerful surface sensitive technique of XPS into an even more powerful technique for performing dynamical measurements which are capable of yielding chemically specific electrical parameters.

References and Notes

(1) Tanaka, K.; Takahara, A.; Kajiyama, T. *Macromolecules* **1996**, *29*, 3232−3239.
(2) Lhoest, J. B.; Bertrand, P.; Weng, L. T.; Dewez, J. L. *Macromolecules* **1995**, *28*, 4631−4637.
(3) Davies, M. C.; Shakesheff, K. M.; Shard, A. G.; Domb, A.; Roberts, C. J.; Tendler, S. J. B.; Williams, P. M. *Macromolecules* **1996**, *29*, 2205−2212.
(4) Clark, M. B.; Burkhardt, C. A.; Gardella, J. A. *Macromolecules* **1989**, *22*, 4495−4501.
(5) Schmitt, R. L.; Gardella, J. A.; Salvati, L. *Macromolecules* **1986**, *19*, 648−651.
(6) Tanaka, K.; Yoon, J. S.; Takahara, A.; Kajiyama, T. *Macromolecules* **1995**, *28*, 934−938.
(7) Bhatia, Q. S.; Pan, D. P.; Koberstein, J. T. *Macromolecules* **1988**, *21*, 2166−2175.
(8) Schmidt, J. J.; Gardella, J. A. *Macromolecules* **1989**, *22*, 4489−4495.
(9) Ton-That, C.; Shard, A. G.; Teare, D. O. H.; Bradley, R. H. *Polymer* **2001**, *42*, 1121−1129.

(10) Ton-That, C.; Shard, A. G.; Daley, R.; Bradley, R. H. *Macromolecules* **2000**, *33*, 8453−8459.

(11) Li, Y. X.; Yang, Y. M.; Yu, F. S.; Dong, L. S. *J. Polym. Sci., Part B: Polym. Chem.* **2006**, *44*, 9−21.

(12) Walheim, S.; Boltau, M.; Mlynek, J.; Krausch, G.; Steiner, U. *Macromolecules* **1997**, *30*, 4995−5003.

(13) Zong, Q.; Li, Z.; Xie, X. M. *Macromol. Chem. Phys.* **2004**, *205*, 1116−1124.

(14) Green, P. F.; Christensen, T. M.; Russell, T. P. *Macromolecules* **1991**, *24*, 252−255.

(15) Takahara, A.; Nakamura, K.; Tanaka, K.; Kajiyama, T. *Mol. Symp.* **2000**, *159*, 89−96.

(16) Mounir, E. S.; Takahara, A.; Kajiyama, T. *Polym. J.* **1999**, *31*, 89−95.

(17) Tanaka, K.; Takahara, A.; Kajiyama, T. *Macromolecules* **1998**, *31*, 863−869.

(18) Dekeyser, C. M.; Biltresse, S.; Marchand-Brynaert, J.; Rouxhet, P. G.; Dupont-Gillain, C. C. *Polymer* **2004**, *45*, 2211−2219.

(19) Kumacheva, E.; Li, L.; Winnik, M. A.; Shinozaki, D. M.; Cheng, P. C. *Langmuir* **1997**, *13*, 2483−2489.

(20) Qu, S.; Clarke, C. J.; Liu, Y.; Rafailovich, M. H.; Sokolov, J.; Phelan, K. C.; Krausch, G. *Macromolecules* **1997**, *30*, 3640−3645.

(21) Dalnoki-Veress, K.; Forrest, J. A.; Dutcher, J. R. *Phys. Rev. E* **1998**, *57*, 5811.

(22) Silva, G. G.; Rocha, P. M. D.; de Oliveira, P. S.; Neves, B. R. A. *Appl. Surf. Sci.* **2004**, *238*, 64−72.

(23) Johnson, W. C.; Wang, J.; Chen, Z. *J. Phys. Chem. B* **2005**, *109*, 6280−6286.

(24) Liu, Y.; Messmer, M. C. *J. Phys. Chem. B* **2003**, *107*, 9774−9779.

(25) Ton-That, C.; Shard, A. G.; Bradley, R. H. *Polymer* **2002**, *43*, 4973−4977.

(26) Artyushkova, K.; Fulghum, J. E. *Surf. Interface Anal.* **2001**, *31*, 352−361.

(27) Suzer, S. *Anal. Chem.* **2003**, *75*, 7026−7029.

(28) Ertas, G.; Demirok, U. K.; Atalar, A.; Suzer, S. *Appl. Phys. Lett.* **2005**, *86*.

(29) Suzer, S.; Dana, A.; Ertas, G. *Anal. Chem.* **2007**, *79*, 183−186.

(30) Suzer, S.; Dana, A. *J. Phys. Chem. B* **2006**, *110*, 19112−19115.